Optica Applicata, Vol. X, No. 4, 1980

Diffraction analysis of the particle size distribution

EUGENIUSZ JAGOSZEWSKI

Institute of Physics, Technical University of Wrocław, Wrocław, Poland.

TADEUSZ PAWLUK

Institute of Industry of Cement Building Materials, Opole, Poland.

In this paper a lens design for beam expansion is presented, and an application of the Keplerian expander to measurement of the particles size distribution is shown. Finally the experimental results made on the designed arrangement are given.

Introduction

This paper is devoted to diffraction analysis of the particle size distribution in four kinds of dust, the preference being given to the cement dust. For this purpose a special arrangement has been designed with a beam expander of Keplerian type as an essential part of it. The first part of the paper deals with the design of the said beam expander, while the further part illustrates its application to the particle size distribution examination based on the method of light scattering. The last part of this work shows the experimental data obtained for quartz flour, talc, fly-ash and cement.

Aberration characteristic of beam expander lens

All optical systems used in applications are subject to aberrations, in particular to spherical aberration, coma, astigmatism, curvature of field, distortion and chromatic aberration. The correction of aberrations depends on the application and for the beam collimating lenses many aberrations become unimportant and their performance is limited mainly by the spherical aberration which can be completely eliminated by using aspherical lenses. This is, however, a rather expensive solution. Therefore, we decided to use a spherical lens version and correct it so that the blur spots be equal to Airy's disc [1].

For our purposes a telescope-objective used to a laser beam expansion has been designed. Assuming the clear aperture of the diameter $D_2 = 50$ mm and the focal length of the lens $f_2 = 500$ mm (i.e. $f/10$), we performed correction for different kinds of glasses, and for wavelength $\lambda = 632.8$ nm of He-Ne laser light. The best solution was obtained by using glasses BK-7 and F-2 (see Schott Catalog [2]). Fig. 1 shows ray-tracing through the designed lens, while fig. 2 shows the graphic representation of longitudinal spherical aberration of the lens. The values of longitudinal spherical

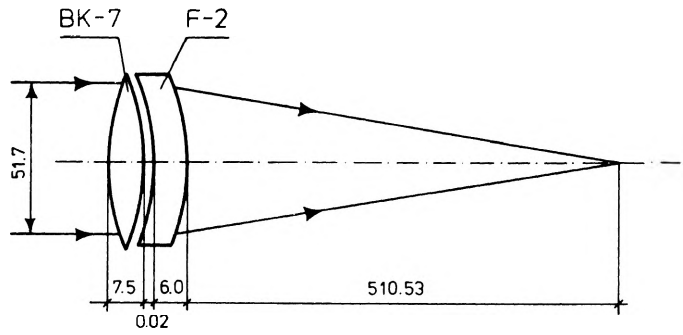

Fig. 1. Telescope-objective of the laser beam expander

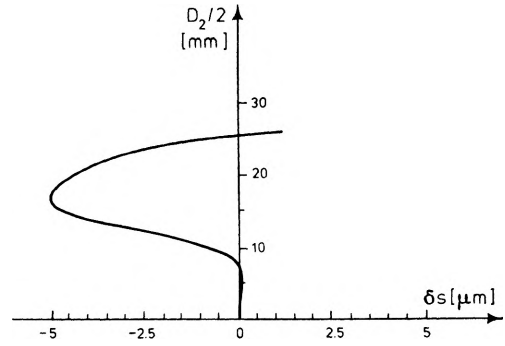

Fig. 2. Longitudinal spherical aberration plotted against intersection of the incident ray with the entrance pupil plane

aberration are presented in the table. We see that the maximum value of the longitudinal spherical aberration tends to the value of 5.5 μm, but we remember that the smallest blur spot lies between two foci: paraxial and marginal ones. For example the smallest blur spot of a single lens lies in a plane which is $^3/_4$ of the distance from the paraxial to the marginal foci. Naturally, the blur spot caused by spherical aberration must not be confused with Airy's disc which is a diffraction pattern produced by the circular aperture. The exact value of focal length of the desired lens is $f_2 = 517.22$ mm.

Table

$D_2/2$ [mm]	δs[mm]
25.861	+0.000402
22.396	−0.003983
18.287	−0.005490
12.931	−0.004147
0.013	+0.000016

Application of a Keplerian expander to a measuring arrangement for particle size distribution

In our consideration a Keplerian telescope system in reverse is used as a laser beam expander. Spatial filtering consists in placing a small pinhole at the common focus of the eye-piece and the objective of a Keplerian system, in which a microscope objective takes place of the Keplerian telescope eye-piece. In this manner the pinhole eliminates the transmission of scattered or multiple-reflected rays. The optimum spatial filter location will be found by experimentation. An optical system for spatial filtering is presented in fig. 3. It is a Fourier transform imaging system in which

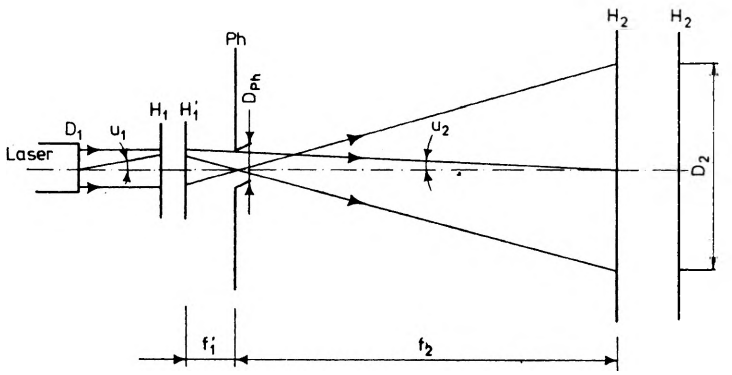

Fig. 3. Schematic diagram of a Keplerian expander

the data located in the front focal plane of a Fourier transform lens of focal length f_1 are imaged in the back focal plane of an inverse Fourier transform lens of focal length f_2. This system is, simultaneously, an expander for laser beam expansion, since two positive lenses are used to change the diameter of a laser beam without affecting its collimation.

If the laser beam has the diameter D_1 and its image formed by microscope objective in the entrance pupil of the telescope objective is D_2, then the whole radiation energy of the laser beam falls at a cross-section plane of the diameter D_2, and the linear magnification is given by

$$M = \frac{D_2}{D_1} = \frac{u_1}{u_2}. \tag{1}$$

The product of the diameter of laser beam and its diverging angle for a given laser is constant [3] and called laser constant

$$D_1 u_1 = D_2 u_2 = \ldots = C. \tag{2}$$

Thus, for a He-Ne laser beam of the wavelength $\lambda = 632.8$ nm and of diverging angle $u = 30''$, the laser constant takes the value $C = 0.20$ μm.

The diameter of a pinhole of the expander can be calculated from the following expression

$$D_{Ph} = 2C\frac{f_2}{D_2}. \tag{3}$$

For our expander having the telescope lens $f/10$, shown in the next section we obtain a pinhole with diameter $D_{Ph} = 5.8$ μm. The inverse Fourier transform lens of the expander, which consists of a diverging and a converging lens, forms an image of the pinhole transparency in the infinity. The expanded laser beam leaves the expander passing through the investigated object transparency and formes a spectrum light distribution in the back focal plane of the next lens.

Let the object plane have N apertures of identical size, shape and orientation. If the aperture was reduced in size to a single point, the irradiance over a plane perpendicular to the direction of wave propagation at a large distance from the aperture would be uniform. For N apertures we must add the respective fields, and by assuming that no appraciable phase shift is involved when different points within the same aperture are considered, we get the irradiance

$$I = I_0|G|^2. \tag{4}$$

That means that on the plane considered the complex light amplitude at the fixed time is given by

$$U = A\exp[i(\varphi - \omega t)]\sum_{n=1}^{N}\exp[-ik(x_n\sin\alpha + y_n\cos\beta)], \tag{5}$$

where $k = 2\pi/\lambda$. A is a constant, φ is a phase angle which varies with the positions of the aperture and the observation point, (x_n, y_n) are the coordinates of the point of the n-th aperture, and α, β are the angles of diffracted ray with the $0x$ plane and the $0y$ plane, respectively [4]. Combining eq. (5) with eq. (4), we obtain the modulation function

$$G(x_n, y_n) = \sum_{n=1}^{N}\exp[-ik(x_n\sin\alpha + y_n\cos\beta)]. \tag{6}$$

Clearly, irradiance defined by eq. (4) combines light beams from all the apertures of the object transparency and represents the time-average value of the energy falling on a unit area of a plane perpendicular to the direction of the wave propagation. It is the average time of the Poynting vector, while the irradiance I_0 represents the time average of the Poynting vector at the observation plane, after the light passed only through the central aperture, located at the optical axis of the system.

Experimental results

In experiments performed on the proposed device all the measurements have been made by means of a silicon photoelement, the sensitive area of which was located in the back focal plane of the objective L_3 (fig. 4). The measurement idea consists in investigation of the diffracted light distribution on the searched objects, taking advantage of the Fraunhofer diffraction effect. L_1 and L_2 (in fig. 4) denote the respective microscope and the designed telescope objectives of the expander, L_3 is an objective

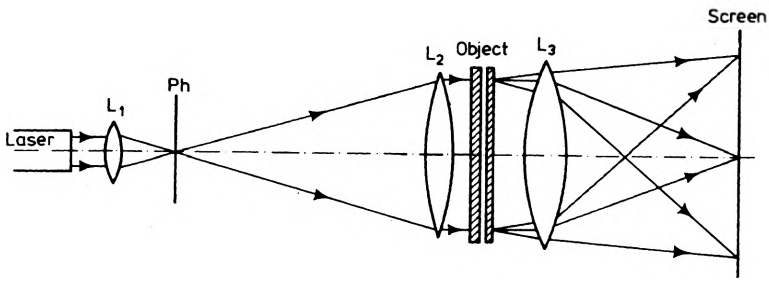

Fig. 4. Schematic diagram of the measurement arrangement for size distribution of particles

of the f-number $f/4.5$, and of the focal length $f = 360$ mm with well corrected aperture and field aberrations. In its back focal plane there are formed the diffraction pattern of light diffracted on the examined particles inserted in the object plane shown in fig. 4.

The figures 5a, b, c, and d represent the intensities of the diffraction pattern vs. the distance from the optical axis measured in the back focal plane of lens L_3. The measurements have been done by a detector of silicon photo element with a sensitive area of the diameter of 0.5 mm. In the object plane (fig. 4) $N = 6000$ apertures of opaque rings identical in shape were inserted. The four pairs of curves in fig. 5 correspond to four different sizes of the investigated apertures.

The figure 6 shows the readings of the detector as a function of the distance of sensitive area from the optical axis for the polydispersive particles of cement. In the top of this figure we see four different object fields: 1/4, 1/2, and 3/4, and the full field of the investigated object plane of cement particles. The field corresponds to the respective four curves in fig. 6.

The figures 7a and b illustrate the voltage of photoelement as a function of the number N of apertures for four different sizes of aperture. The voltage of the photoelement has been measured at a fixed distance of the detector from the optical axis of the device. In fig. 7a and b the distances between the position of the detector and the point of intersection of the optical axis with the back focal plane of lens L_3 are equal to $r = 1.0$ mm and $r = 1.5$ mm, respectively.

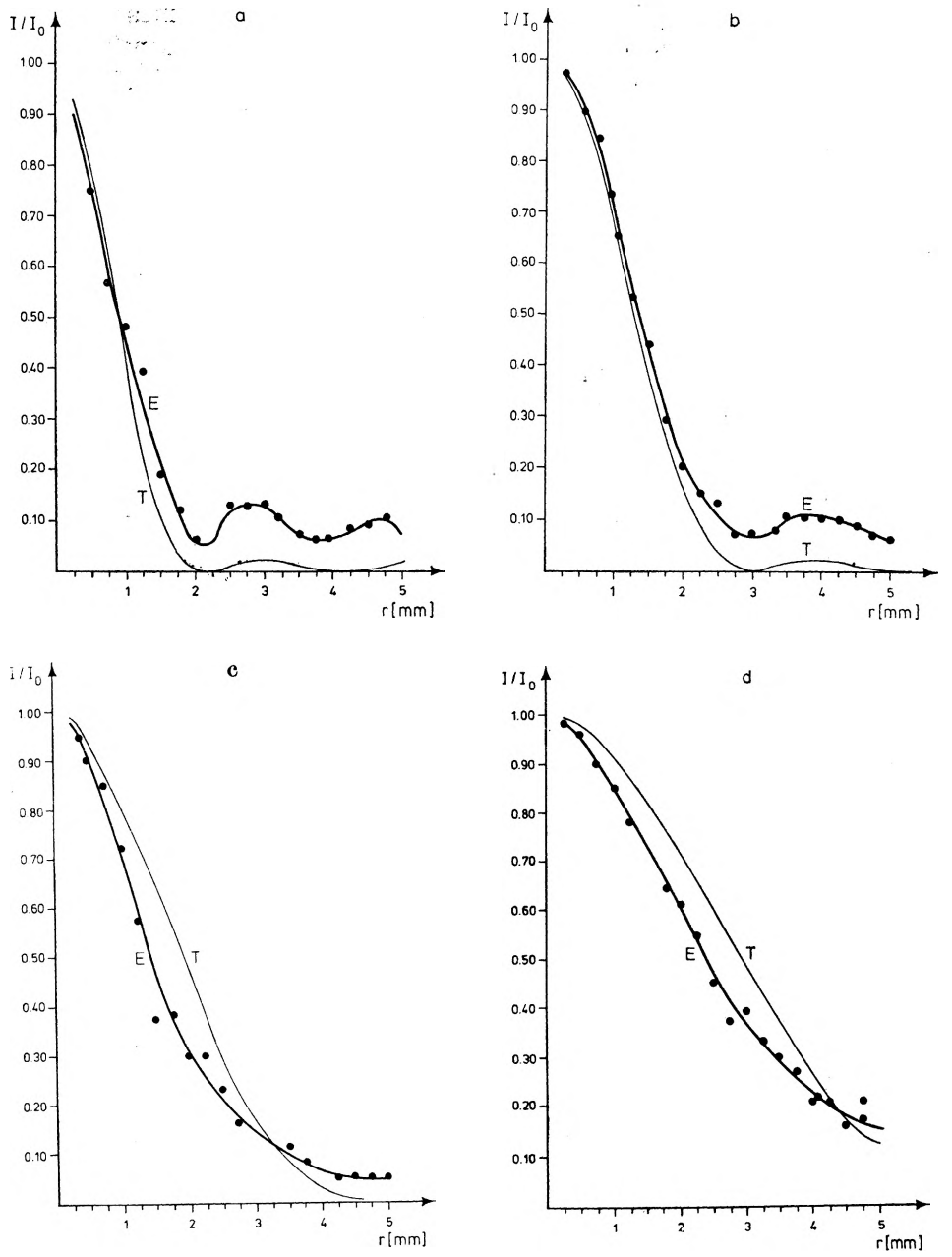

Fig. 5. The ratio of the intensity to the maximum intensity as a function of the distance from the optical axis in the back focal plane of lens L_3

E – experimental curve, T – theoretical curve. The measurements are made for $N = 6000$ apertures of diameters: (a) ⌀ 129 μm, (b) ⌀ 90 μm, (c) ⌀ 60 μm, (d) ⌀ 40 μm

The figure 8 represents the voltage of the photoelement as a function of the distance between the position of the detector and the point of intersection of the optical axis with back plane of the lens L_3 for the polydispersive particles with different composition of grain. In composi-

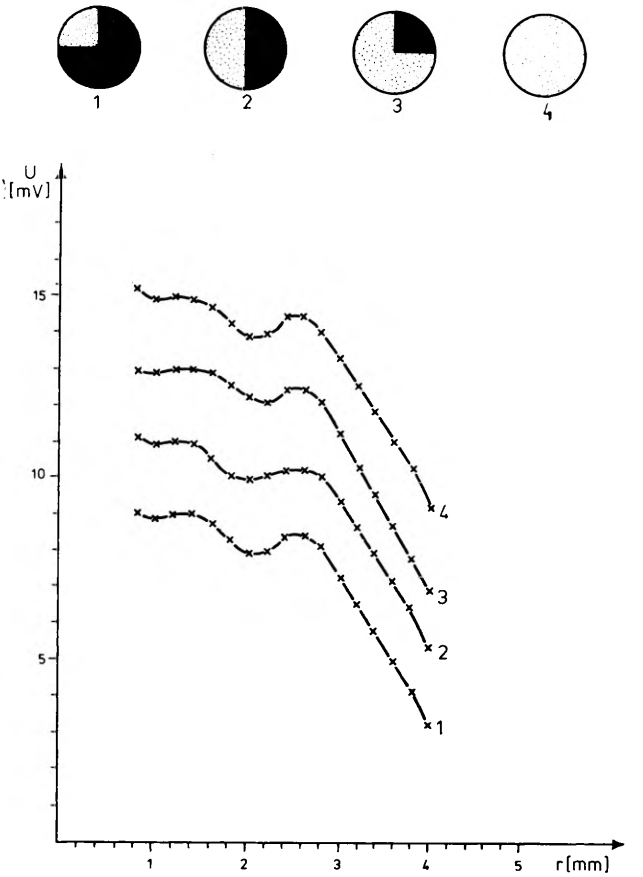

Fig. 6. The readings of the detector as a function of the distance from the optical axis

The experimental curves 1, 2, 3, and 4 correspond to the object fields 1, 2, 3, and 4, rescpetively

tion (I) there is a large number of small particles (88.3 %), while in the composition (II) the bigger particles prevail (80.5 %).

Finally, fig. 9 shows the dependence of intensity of the diffraction pattern on the rotation of the object plane by a fixed distance between

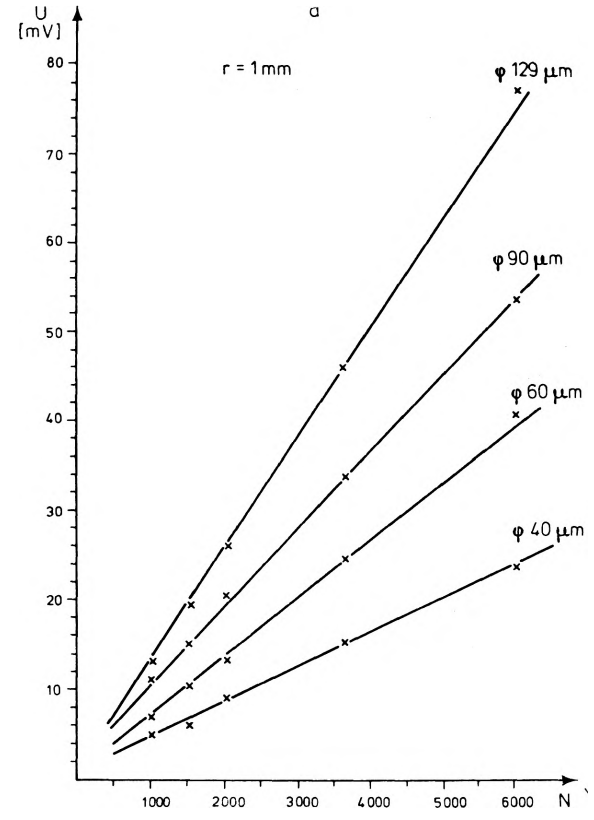
a
U
[mV]
r = 1 mm
φ 129 µm
φ 90 µm
φ 60 µm
φ 40 µm
80
70
60
50
40
30
20
10
1000
2000
3000
4000
5000
6000
N

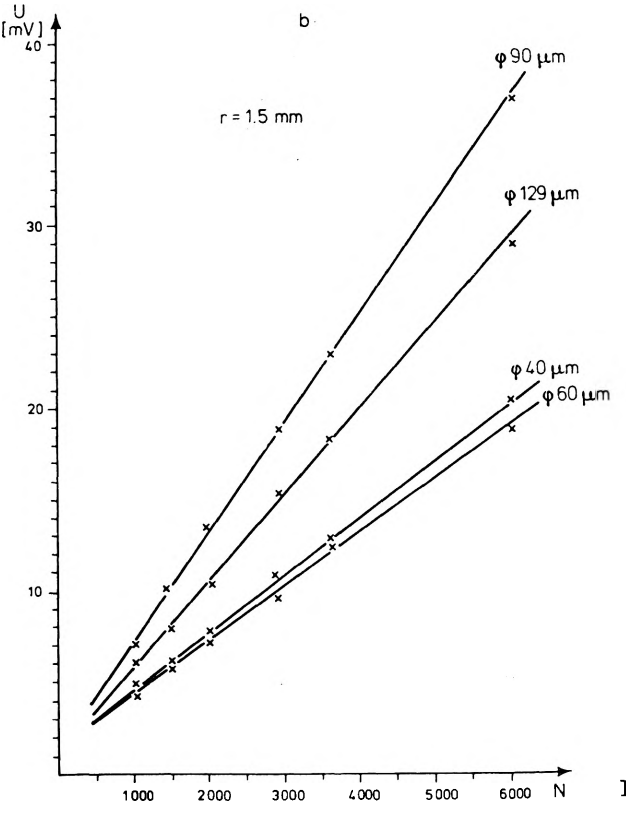
b
U
[mV]
r = 1.5 mm
φ 90 µm
φ 129 µm
φ 40 µm
φ 60 µm
40
30
20
10
1000
2000
3000
4000
5000
6000
N

Fig. 7

the detector and the intersection point of the optical axis with back focal plane of the lens L_3. The measurements have been performed for four different materials with fixed composition, and for each material in four fixed positions of the detector (namely: $r = 0.8$, 1.0, 2.0, 3.0 mm). The object plane has been turned about the axis of the optical system by the values of angle $\pi/4$ from 0 to 2π radians. The four curves (I, II, III, IV) in each figure have almost the axial symmetry. These are some insignificant deviations from the full axial symmetry caused rather by irregularity of the distribution of particles than by their polarization in a determined direction. Fig. 10 shows a photography of the arrangement used for examination of the Fraunhofer diffraction effects.

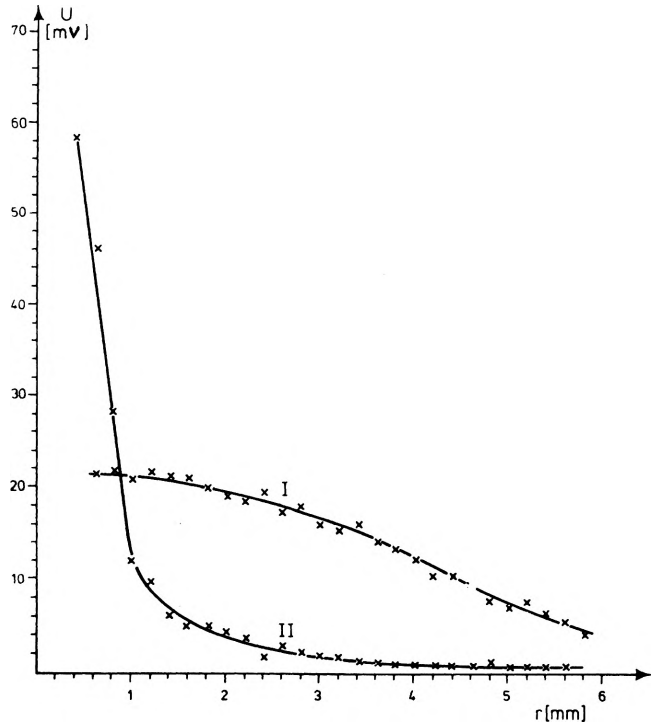

Fig. 8. The voltage of the photoelement as a function of the distance between the position of detector and of the intersection point of the optical axis with the measurement plane for two different compositions of grain

I. lower than 3 μm – 88.3 %, 3-10 μm – 7.0 %, 10-20 μm – 3.3 %, 20-30 μm – 1.0 %, 30-60 μm – 0.4 %;
II. lower than 3 μm – 1.3 %, 3-10 μm – 1.7 %, 10-20 μm – 4.0 %, 20-30 μm – 12.5 %, 30-60 μm – 80.5 %

Fig. 7. The voltage of the photoelement as a function of the number of apertures of the diameters ⌀40 μm, ⌀60 μm, ⌀90 μm, and 129 μm

The measurements are made for two fixed distances between the position of detector and the point of intersection of optical axis with the back focal plane of L_3: (a) $r = 1.0$ mm, (b) $r = 1.5$ mm

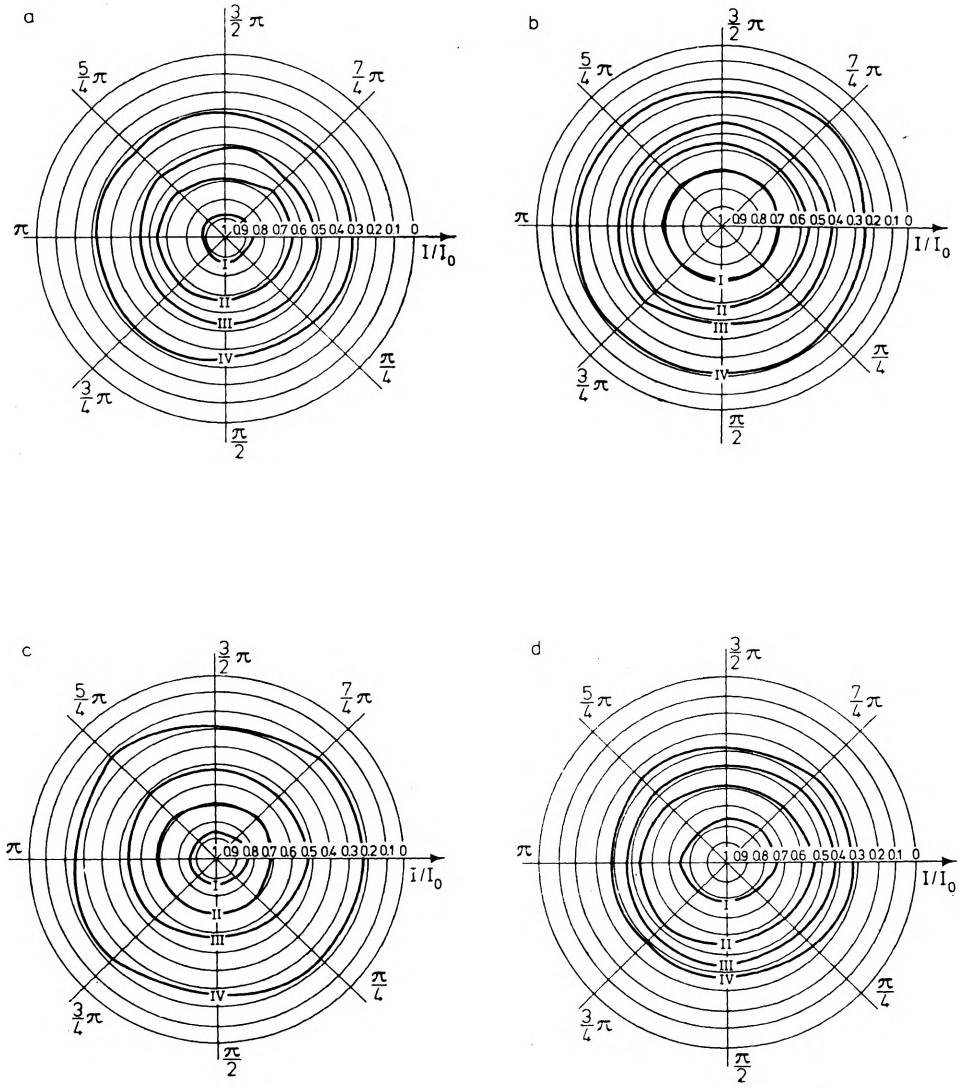

Fig. 9. The ratio of the intensities I/I_0 as a function of rotation of the object plane by fixed distance of the detector from the optical axis. Investigated materials:

(a) quartz flour: lower than 3 μm – 18 %, 3-10 μm – 14 %, 10-20 μm – 12 %, 20-30 μm – 13 %, 30-60 μm – 21 %; higher than 60 μm – 22 %; I r = 0.8 mm II r = 1.0 mm III r = 2.0 mm IV r. = 3.0 mm
(b) talc: lower than 3 μm – 32 %, 3-10 μm – 22 %, 10-20 μm – 23 %, 20-30 μm – 17 %, 30-60 μm – 5 %; higher than 60 μm – 1 %; I r = 0.8 mm, II r = 1.0 mm, III r = 2,0 mm, IV r = 3.0 mm
(c) fly ash: lower than 3 μm – 16 %, 3-10 μm – 10 %, 10-20 μm – 13 %, 20-30 μm – 21 %, 30-60 μm – 19 %; higher than 60 μm – 21 %; I r = 0.8 mm, II r = 1.0 mm, III r = 2.0 mm, IV r = 3.0 mm
(d) cement: lower than 3 μm – 7 %, 3-10 μm – 17 %, 10-20 μm – 20 %, 20-30 μm – 21 %, 30-60 μm – 22 %; higher than 60 μm – 13 %; I r = 0.8m m, II r = 1.0 mm, III r = 2.0 mm, IV r – 3.0 mm

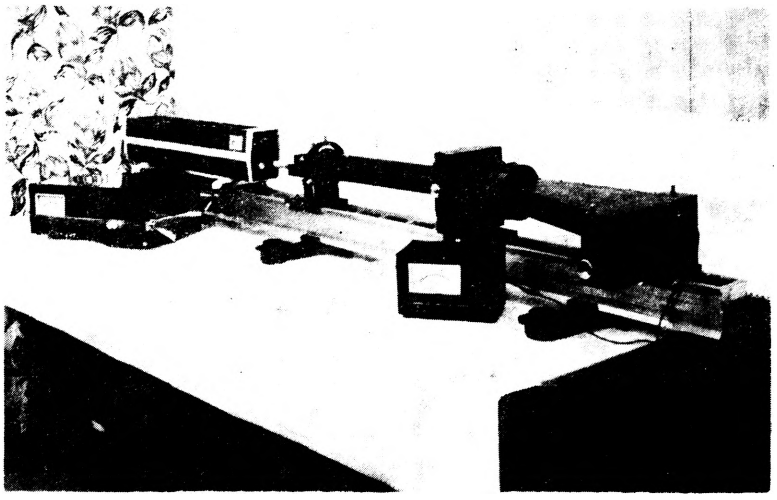

Fig. 10. The arrangement for examination of the Fraunhofer diffraction effects

Conclusions

The expander described here and used in the arrangement to examine the Fraunhofer diffraction effects can be applied to measurement of the sizes of small particles. From a number of experiments performed in a sample of particles and materials with different grains it may be concluded that this arrangement will be suitable for investigations and measurements of both the particles size distributions and the grain composition.

References

[1] Born M, Wolf E., *Principles of Optics*. 2-nd rev. ed., Pergamon Press, New York 1964.
[2] Schott Catalog: Optical Glass, Spezial-Glas, GmBH Mainz.
[3] Jagoszewski E., Flasiński Z., *Granulometr laserowy*, Report No. 321/78, Institute of Physics, Technical University of Wrocław, Wrocław 1978.
[4] Yu F. T. S. *Introduction to Diffraction, Information Processing, and Holography*, Massachusetts Institute of Technology Press, Massachusetts 1973.

Received December 6, 1979,
in revised form January 27, 1980

Дифракционный анализ распределения величины частиц

Описано устройство для исследования распределения величины частиц избранных пластических материалов. Приложенная аберрационная характеристика телеобъектива расширителя лазерного пучка свидетельствует о подборе проведенной коррекции этого объектива для типовых оптических стёкол. Проведенные опыты дифракций Фраунхофера на различных фракциях зёрен пылей проиллюстрированы соответствующими графиками